Genetic Evolution of Glioblastoma Stem-Like Cells From Primary to Recurrent Tumor

UNIVERSITÀ DEGLI STUDI DI TORINO

Genetic Evolution of Glioblastoma Stem-Like Cells From Primary to Recurrent Tumor

Francesca Orzan[1], Francesca De Bacco[1], Giovanni Crisafulli[2,3], Serena Pellegatta[4], Benedetta Mussolin[2], Giulia Siravegna[2], Antonio D'Ambrosio[1,3], Paolo M. Comoglio[1], Gaetano Finocchiaro[4], Carla Boccaccio[1,3]

[1]Laboratory of Cancer Stem Cell Research, Candiolo Cancer Institute, FPO-IRCCS, Candiolo, Italy.
[2]Laboratory of Molecular Oncology, Candiolo Cancer Institute, FPO-IRCCS, Candiolo, Italy.
[3]Department of Oncology, University of Torino, Candiolo, Italy.
[4]Unit of Molecular Neuro-Oncology, Fondazione IRCCS Istituto Neurologico C. Besta, Milan, Italy.

Abstract

Glioblastoma (GBM) is a lethal tumor that displays remarkable genetic heterogeneity. It is also known that GBM contains a cell hierarchy driven by GBM stem-like cells (GSCs), responsible for tumor generation, therapeutic resistance, and relapse. An important and still open issue is whether phylogenetically related GSCs can be found in matched primary and recurrent GBMs, and reflect tumor genetic evolution under therapeutic pressure. To address this, we analyzed the mutational profile of GSCs isolated from either human primary GBMs (primary GSCs) or their matched tumors recurring after surgery and chemoradiotherapy (recurrent GSCs). We found that recurrent GSCs can accumulate temozolomide-related mutations over primary GSCs, following both linear and branched patterns. In the latter case, primary and recurrent GSCs share a common set of lesions, but also harbor distinctive mutations indicating that primary and recurrent GSCs derive from a putative common ancestor GSC by divergent genetic evolution. Interestingly, TP53 mutations distinctive of recurrent GSCs were detectable at low frequency in the corresponding primary tumors and likely marked pre-existent subclones that evolved under therapeutic pressure and expanded in the relapsing tumor. Consistently, recurrent GSCs displayed in vitro greater therapeutic resistance than primary GSCs. Overall, these data indicate that (a) phylogenetically related GSCs are found in matched primary and recurrent GBMs and (b) recurrent GSCs likely pre-exist in the untreated primary tumor and are both mutagenized and positively selected by chemoradiotherapy. Stem Cells 2017;35:2218–2228

Significance Statement

Glioblastomas (GBMs) encompass genetically heterogeneous tissue areas, reflecting the presence of distinct cell subclones. These subclones can be differentially selected by standard chemoradiotherapy and give rise to genetically evolved, therapeutically resistant recurrences. To better understand the therapeutic response and the mechanisms of progression, the evolutionary dynamics of GBM subclones should be deciphered at the level of GBM stem-like cells (GSCs), that is, the often minor cell subpopulation that originates each subclone. The results of this study show for the first time that GSCs from recurrent GBMs are phylogenetically related with those prevailing in the primary tumor, are pre-existing to therapy, and evolve under therapeutic pressure.

Introduction

In most glioblastoma (GBM) patients, tumor control achieved by the standard protocol, combining surgery, chemoradiotherapy, is followed by a rapid tumor recurrence that is lethal within 12–15 months after the first diagnosis [1]. Recurrence implies that, in the primary tumor, at least one subclone survives therapy, takes advantage from elimination of coexisting subclones and propagates. Several genetically distinct subclones are usually present in the same GBM, harboring different assortments of a handful of driver genes [2-4]. If these subclones display different responses to therapies, that is, they subside or survive based on their genetic differences, then tumor genetic evolution should occur under therapeutic pressure and become evident by comparing primary and recurrent tumor. Deciphering this evolutionary dynamics is relevant to predict the disease course and to understand the causes of therapeutic failure, that is, the mechanisms by which the immediate benefit (therapeutic sensitivity) is followed by the detrimental long-term positive selection of refractory subclones (therapeutic resistance). So far, few studies have addressed this issue by undertaking longitudinal genetic analysis of primary GBMs and their recurrences. These studies revealed that GBM contains complex subclonal architectures that evolve under therapy [5-8]. However, it is still unknown whether therapy-

driven genetic evolution occurs in GBM stem-like cells (GSCs). Indeed, this subpopulation is inherently resistant to chemoradiotherapy as a whole, as compared to the non-stem subpopulation [9-11], but it includes GSCs endowed with distinct genetic and functional properties, which could underlie different therapeutic sensitivity [12-14]. Here, by a retrospective analysis of GSCs isolated from matched primary and recurrent GBMs, we investigated whether phylogenetically related but distinct GSCs can coexist within the primary tumor and can be differentially selected by the evolutionary pressure imposed by therapies.

Materials and Methods

Neurosphere Derivation and Culture

Four neurosphere (NS) pairs (Supporting Information Table S1) were derived from matched primary and recurrent GBMs provided by Surgical Departments at the Fondazione IRCCS Istituto Neurologico C. Besta (Milan), according to the ethical requirements of the institutional committee on human experimentation. Informed consent was obtained from all individual participants included in the study. Tumors were defined as “de novo GBM” at the time of the first surgery, according to World Health Organization criteria [15].

NS were derived by mechanical dissociation and digestion of tumor specimens with collagenase type I (ThermoFisher, Waltham, MA, USA). Single-cell suspensions were plated at clonal density (1–10 cells per microliter) in standard medium containing: Dulbecco's modified Eagle's medium/F-12 (ThermoFisher), 2 mM glutamine (Sigma, St. Louis, MO, USA), penicillin–treptomycin (1:100, Sigma), B-27 (1:50, ThermoFisher), human recombinant epidermal growth factor, and basic fibroblast growth factor (20 ng/ml each; Peprotech, London, UK). During the initial passages, medium was replaced or supplemented with fresh growth factors until cells started to grow forming floating aggregates. To expand cultures, spheres were mechanically dissociated, counted with trypan blue to evaluate the number of live cells, and then replated as single cells at clonal density in complete fresh medium. Cells were incubated at 37°C, 5% CO_2, and H_2O saturated atmosphere. NS cultures were defined as established and self-propagating after 15 passages, and cells were analyzed between 15 and 20 passages.

For single cell cloning, 120 cells were sorted from NS and directly seeded by MoFlo Astrios Cell Sorter (Beckman Coulter, Brea, CA, USA) into two 96-well plates (1 cell per well) in standard medium. The obtained sub-clones were expanded in vitro and used for nucleic acid extraction.

Nucleic Acid Extraction

From established NS, nucleic acids were extracted using the AllPrep DNA/RNA mini kit (Qiagen, Hilden, Germany), according to manufacturer's instructions. DNA from formalin fixed paraffin embedded (FFPE) tumor tissues was extracted using PureLink Genomic DNA Mini Kit (ThermoFisher) according to manufacturer's instruction. Nucleic acids were quantified with Nanodrop ND1000 (ThermoFisher) and used as described below.

O-6-Methylguanine-DNA Methyltransferase Expression Analysis

cDNA was obtained with the High-Capacity cDNA Reverse Transcription Kit (ThermoFisher) using 150 ng of total RNA. Real-time polymerase chain reaction (PCR) was performed using primer and probe sets for O-6-methylguanine-DNA methyltransferase (MGMT) (Hs01037698_m1), TaqMan PCR MasterMix, and an ABI PRISM 7900HT sequence detection system (ThermoFisher). beta-2 microglobulin (β2M) (Hs00984230_m1) was used as control. Only samples with undetectable levels of MGMT were considered as MGMT negative.

NS Pair Authentication

Fingerprint analysis was performed by GenePrint 10 System (Promega, Madison, WI, USA) following manufacturer's instruction. Briefly, amplicons from multiplex PCR products including 10 human loci (TH01, TPOX, VWA, AMELX, CSF1PO, D16S539, D7S820, D13S317, D5S818, and D21S11) were separated on a

3730 DNA Analyzer (ThermoFisher). Allele call was performed with GeneMapperID software (ThermoFisher). NS pair authentication was also confirmed by single nucleotide polymorphism identification (SNP ID) on next generation sequencing (NGS) data.

Gene Copy Number Analysis

Gene copy number of cyclin dependent kinase inhibitor 2A (CDKN2A), phosphatase and tensin homolog(PTEN), platelet-derived growth factor receptor A (PDGFRA), epidermal growth factor receptor (EGFR), MYC proto-oncogene (MYC), hepatocyte growth factor (HGF), and hepatocyte growth factor receptor(MET) was assessed by real-time PCR, using TaqMan Copy Number Assays (ThermoFisher) and the ABI PRISM 7900HT sequence detection system (ThermoFisher). Relative gene copy number data were calculated by normalizing against endogenous controls (GREB1 and RPPH1). The copy number of each gene was calculated with the formula $2 \times 2^{-\Delta\Delta Ct}$ using a normal diploid human genomic DNA (gDNA) as calibrator. Homozygous deletion was defined by lack of PCR amplification of the target gene in the presence of PCR product for control probes; heterozygous deletion was defined by a copy number <1.5; a copy number between 1.5 and 3 was considered as normal. PDGFRA was considered amplified with a copy number higher than 5. To discriminate between real EGFR or MET amplification, and polysomy of chromosome 7 (harboring the two genes), the calculated copy number was normalized against the copy number of another gene (HGF) mapped on the same chromosome and usually not amplified. For each sample, we defined as “true amplification” a copy number of EGFR or MET at least sixfold higher than that of HGF (amplification threshold). A copy number included between 3 and the amplification threshold was considered as copy number gain.

Sanger Sequencing

PCR conditions and oligos for tumor protein P53 (TP53) and IDH1 (exon 4) were as described [16]. PCR products were purified using ExoSAP-IT (ThermoFisher) according to manufacturer's instruction. Cycle sequencing was carried out using BigDye Terminator v3.1 Cycle Sequencing kit (ThermoFisher). Sequencing products were purified using AgencourtCleanSeq (Beckman Coulter) and analyzed on a 3730 DNA Analyzer (ThermoFisher). Sequences were then analyzed using Chromas Lite 2.01 software (http://www.technelysium.com.au/chromas_lite.html) and compared with reference sequences from the Homo sapiens assembly GRCh37. TP53 cloning was performed on two independent subclones of #3 and #4 recurrences by TOPO-TA cloning kit (ThermoFisher) following standard procedures. For each subclone, at least six colonies were transferred into 0.2 ml of fresh lysogeny broth medium plus ampicillin and incubated for 1 hour at 37°C. Five microliters of these suspensions were transferred in 50 μl of water, incubated for 10 minutes at room temperature (RT) and lysed at 95°C for 5 minutes. Two microliter of lysate was then used as template for TP53 PCR amplification and sequencing as described above.

Next Generation Sequencing

Libraries were prepared with Nextera Rapid Capture Custom Enrichment Kit (Illumina Inc., San Diego, CA, USA), according to the manufacturer's protocol. Briefly, preparation of libraries was performed starting from 100 ng of gDNA. gDNA was fragmented using transposons, adding simultaneously adapter sequences. Purified tagmented gDNA was used as template for subsequent PCR to introduce unique sample indexes. The size distribution of the DNA fragments was assessed using the 2100 Bioanalyzer with the High Sensitivity DNA assay kit (Agilent Technologies, Santa Clara, CA, USA). Equal amounts of DNA libraries were pooled and subjected to hybridization capture on a custom target panel (“IRCC target panel”) including 226 cancer-associated genes (Illumina Inc.), as described previously [17]. Libraries were then sequenced using an Illumina MiSeq sequencer (Illumina Inc.).

Bioinformatic Mutational Analysis

Mutational discovery analysis was performed by an updated version of an already published and described NGS pipeline [17], to call somatic variations and indels. To discard sequencing artifacts that could alter transition/transversion in samples treated with temozolomide [18], high-depth NGS data were further filtered resulting in a final median depth of 274× (eight samples), with more than 98.5% of the targeted region covered by at least 10 reads. The following filters were applied: (a) all low-quality nucleotides in fragments with Phred Score < 30 were discarded; (b) all mutations

supported by reads having a strand bias, or by a mismatch only in head/tail of the read were disregarded; (c) only mutations with 5% significance level (Fisher's exact test) and at least 10% allelic frequency were considered reliable. Aligned reads having more than three mismatches and genes having more than 10 mutations were excluded. Germline mutations were annotated from the complete list of reported mutations from Single Nucleotide Polymorphism Database (vers. 147). To identify temozolomide-associated mutational signatures in recurrent NS, the recurrent-specific genetic variations were analyzed according to ref. [19].

Biological Assays

Approximately 10^3 cells per well were plated in a 96-well plate at day 0, cells were treated, and viability was measured by CellTiter-Glo Luminescent Cell Viability Assay (Promega) using a GloMax 96 Microplate Luminometer (Promega) as detailed below. Cell proliferation rate was evaluated at 1, 4, 7, and 10 days after seeding. To evaluate cell response to radiation, cells were irradiated with a 200-kV X-ray blood irradiator (Gilardoni, Lecco, Italy), operating at RT, and with a 1 Gy/minute dose rate, with a dose of 2 Gy administered for three consecutive days. Cell viability was measured 1, 4, and 7 days after the last dose. To evaluate cell response to chemotherapy, cells were treated with temozolomide (Sigma) with 5 to 50 μM three times, every 3 days. Cell viability was measured 1, 4, 7, and 10 days after seeding. Data are reported as mean ± SEM of at least two independent experiments in six replicates.

In Vivo Tumorigenicity

All animal procedures were approved by the internal Ethical Committee for Animal Experimentation and by the Italian Ministry of Health. To evaluate tumorigenicity, 2×10^5 dissociated NS cells were resuspended in 100 μl v/v phosphate-buffered saline/Matrigel (BD Biosciences, San Jose, CA, USA) and injected subcutaneously in the right flank of 6–8 weeks old male NOD.CB17-Prkdcscid/NcrCr mice (n = 5 per group) (Charles River Laboratories, Wilmington, MA, USA). Tumor diameters were measured every week by caliper, and tumor volume was calculated using the formula: $4/3\pi \times (d/2)^2 \times (D/2)$, where dand D are the minor and the major tumor axis, respectively. An average tumor volume of 1,000–1,200 mm^3 for each group was considered as the experimental endpoint.

Droplet Digital PCR

The search for low-frequency specific mutations was carried out by droplet digital PCR (ddPCR) as follows: DNA isolated from paraffin-embedded tumor tissues or NS was amplified using ddPCR Supermix for Probes (Bio-Rad, Hercules, CA, USA) using TP53 G245D, T253I, T211I and A189T probes (Bio-Rad). ddPCR was then performed according to manufacturer's protocols as described [20].

Statistical Analysis

Values were expressed as mean ± SEM. Statistical analyses were performed using GraphPad Prism Software (GraphPad Software Inc., La Jolla, CA, USA). Unpaired two-sided Student's t test or Mann Whitney test was used as indicated. A $p < .05$ was considered to be significant.

Results

Genetic Analysis of GSCs (NSs) Derived from Primary and Recurrent GBM Tissues

We reasoned that, when genetic evolution occurs during GBM progression, GSCs found in the recurrent tumor should be genetically distinct from those found in the primary. At the same time, given the likely monoclonal origin of the tumor, these GSCs should be also phylogenetically related and display signs of either linear of divergent accumulation of genetic lesions.

To test this hypothesis, we performed a retrospective analysis of four GBM cases (#1–4, Fig. 1A). NS, that is, cultures enriched in stem/progenitor cells, were established from surgical fragments of matched primary and recurrent tumors. In all cases, one NS was obtained from the primary GBM (“primary NS”). A second NS (“recurrent NS”) was derived from

the recurrent GBM, arising in the same patient after the first line of chemo- and/or radiotherapy (cases #1–3, Fig. 1B), or after a second surgery and a further line of therapy with the anti-vascular endothelial growth factor antibody bevacizumab (case #4, Fig. 1C). The presence of a wild-type IDH1 gene in all NS confirmed the clinical diagnosis of de novo GBM [1]. Matched primary and recurrent NS were verified to derive from the same patient by fingerprint analysis and further confirmed by SNP ID (Supporting Information Tables S2, S3A–S3E).

A

CASE ID	SEX	AGE (year)	LOCATION			PFS (months)	OS (months)	TREATMENT	
			primary	recurrent	recurrent II			1st	2nd
#1	M	49	T left	T left	-	9	18	RT+TMZ	-
#2	M	58	T right	T right	-	9.5	22.5	RT+TMZ	-
#3	M	45	T left	T right	-	14	23	TMZ‡CARM	-
#4	F	33	F right	F right	F right	6	30	RT+TMZ	BEV

B

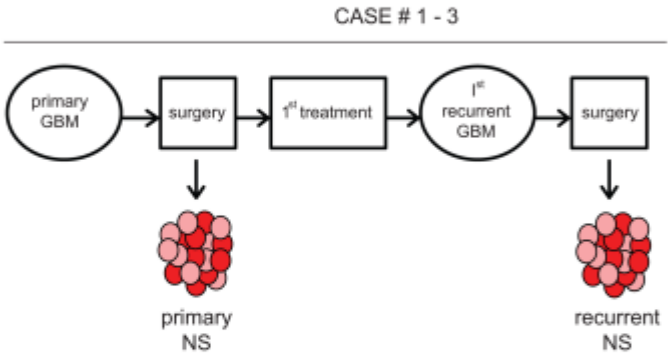

C

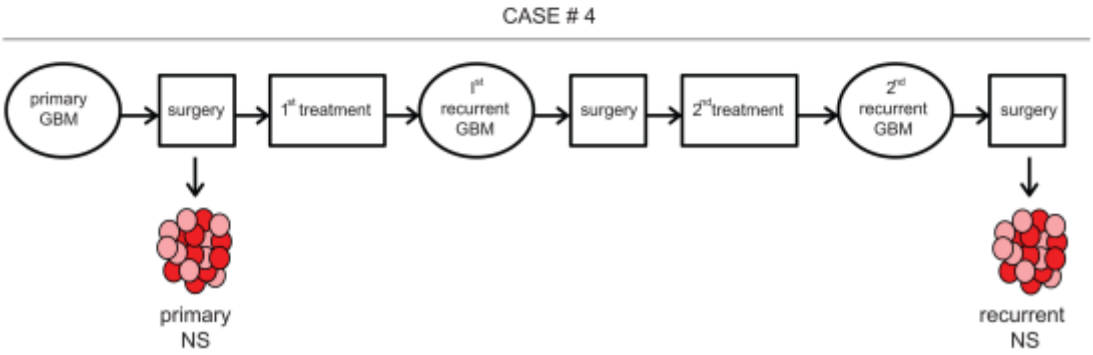

Figure 1. Clinical features and overview of neurosphere (NS) derivation. (A): Clinical features of glioblastoma cases #1–4. (B, C): Schematic representation of NS derivation with respect to the treatments in cases #1–3 (B) and #4 (C). Abbreviations: GBM, glioblastoma; NS, neurosphere; PFS: progression free survival (months); OS: overall survival (months); Location: T (temporal); F (frontal); Treatment: RT: radiotherapy; TMZ: Temozolomide; CARM.: carmustine; BEV: Bevacizumab; a: Temozolomide two cycles, suspended for toxicity.

All NS displayed the features of GSCs, namely, self-renewal, clonogenicity, and tumorigenicity, as they could propagate in vitro at clonal density for an indefinite number of passages, and generated tumors that phenocopied the originals after transplantation in immunocompromised mice (Supporting Information Fig. S1 and data not shown).

The mutational profile of NS pairs was analyzed by NGS of a custom target panel of 226 cancer-related genes (IRCC target panel [17]), including all relevant GBM genetic drivers. Copy number variations of frequently amplified (EGFR, MET, PDGFRA, MYC) or deleted (CDKN2A and PTEN) genes, as well as expression of MGMT, a negative predictor of therapeutic response to temozolomide, were also assessed by real-time PCR (Fig. 2A; Supporting Information Tables S4–S7) [1].

A

CASE ID	NS ID	COPY NUMBER VARIATION						MUTATED GENES*	*MGMT* expression
		EGFR	*MET*	*PDGFRA*	*CDKN2A*	*PTEN*	*MYC*		
#1	primary	wt	+	wt	wt	-	wt	*DNMT3A, ERBB3, PDGFRA, PTEN, TP53*	+
	recurrent	wt	wt	wt	wt	-	wt	*DNMT3A, ERBB3, PDGFRA, PTEN, TP53*	-
#2	primary	+ +	+	wt	wt	-	wt	*ERBB2*	+
	recurrent	+ +	+	wt	wt	-	wt	*ERBB2*	+
#3	primary	+	wt	wt	- -	-	wt	*PTEN*	-
	recurrent	+	wt	wt	- -	-	+ +	***ASXL1, CCNE1, DDB2, EGFR, GNAS, IKZF1, KMT2A, MSH2, NOTCH4, PIK3R1, PMS2,*** *PTEN,* ***RAF1, TP53***	-
#4	primary	+	wt	wt	- -	-	+ +	*BRCA2, EGFR,* ***TP53***	-
	recurrent	+ +	wt	wt	- -	-	+ +	***APC, AR, ARID1A, ARID1B, BMPR1A,*** *BRCA2,* ***BRIP1, CDC73, CDKN2C, CREBBP,*** *EGFR,* ***EZH2, FANCD2, IGF2R, JAK3, KDR, KMT2A, MED12, MEN1, MPL, MSH6, NF1, NKK2-1, NOTCH1, NOTCH2, NOTCH4, NPM1, NRAS, NSD1, PIK3R1, POLD1, PTEN, RAF1, RNF43, SF3B1, SMAD2, SMO, STAG2, TCF7L2, TP53, TSC1, XPC***	-

B

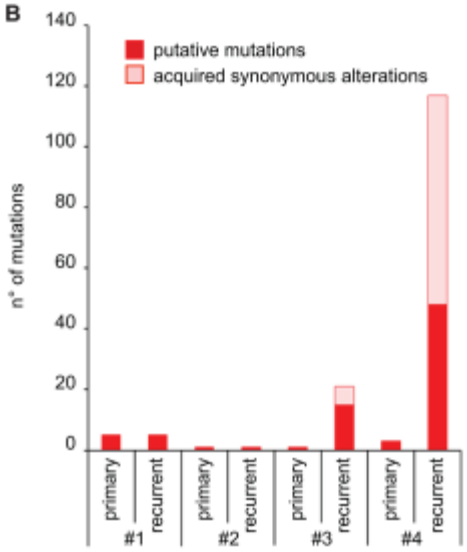

Figure 2.Genetic alterations in matched primary and recurrent neurospheres (NS). (A): Summary of gene copy number variations, mutations found by next generation sequencing (as detailed in Supporting Information Tables S4–S7), and O-6-methylguanine-DNA methyltransferaseexpression. (B): Number of mutations called for each primary and recurrent NS sample. Putative mutations are alterations not described as single nucleotide polymorphisms (SNPs) and affecting protein functions. Acquired synonymous alterations are de novo variations described as SNPs and/or not affecting protein functions. Abbreviation: NS, neurosphere; SNP, single nucleotide polymorphism. Abbreviations: *: alterations not described as SNP and affecting protein functions; ++: amplification; +: copy number gain; -: heterozygous deletion; --: homozygous deletion; wt: absence of copy number variations; bold: gene differentially altered in primary vs recurrent NS.

In two pairs of matched NS (cases #1 and #2), both primary and recurrent NS displayed the same alterations (Fig. 2; Supporting Information Tables S4, S5). Namely, pair #1 harbored PTEN biallelic inactivation, and DNMT3A, ERBB3, PDGFRA, and TP53 mutations, while pair #2 displayed EGFRamplification and an ERBB2 mutation. Both cases harbored an intact CDKN2A gene. Although we cannot exclude that #1 and #2 primary and recurrent NS harbor differences in other loci not included in our analysis, the complete concordance in the sequence of the 226 cancer-related genes included in the target panel, and corresponding to 0.6 MB, strongly suggests that the primary tumor (sub)clone, from which the primary NS was derived, was not fully eradicated by surgery and ensuing chemoradiotherapy. Similarly, the same (sub)clone re-expanded in the patient to generate the relapsing tumor from

which the recurrent NS was derived. This lack of accumulation of genetic alterations, observed in the recurrent NS despite treatment with the alkylating agent temozolomide after surgery (Fig. 1), can be explained by expression of MGMT, as detected in the primary NS (Fig. 2A), which catalyzes the efficient removal of DNA adducts.

On the contrary, in the other two cases (#3 and #4), the recurrent NS accumulate several genetic alterations over the primary NS (Fig. 2A, 2B; Supporting Information Tables S6, S7). Such accumulation was associated with temozolomide treatment in the absence of MGMT expression (Fig. 2A). Indeed, the genetic alterations specific of recurrent NS displayed features overlapping with the previously identified temozolomide signature (Supporting Information Fig. S2) [19]. We thus tried to establish genealogical relationships between primary and recurrent NS of cases #3 and #4, by comparing their respective genetic lesions.

Pair #3: Linear Accumulation of Mutations from Primary to Recurrent GSCs

In pair #3, the recurrent NS retained the only two genetic lesions found in the primary NS (CDKN2Ahomozygous deletion and PTEN biallelic alteration) and acquired 13 additional mutations potentially affecting protein functions and MYC amplification, consistently with a pattern of linear accumulation (Fig. 2A, 2B; Supporting Information Table S6). Interestingly, in the recurrent NS, TP53 displayed two different heterozygous mutations confirmed by Sanger sequencing (Fig. 3A; Supporting Information Table S6A). By analysis of six different cell subclones of the recurrent NS, obtained by single-cell cloning, we could show that the two TP53 mutations coexisted in the same cells. Moreover, by cloning and sequencing the PCR fragment containing the two TP53 mutations, obtained from the above cell subclones, we showed that the two TP53 mutations occurred on distinct alleles (Fig. 3B). Taken together, these analyses indicate that the primary NS represents GSCs from an ancestral tumor clone, whereas the recurrent NS represents GSCs from a subclone which evolved from the ancestral by linear accumulation of mutations (Fig. 3C).

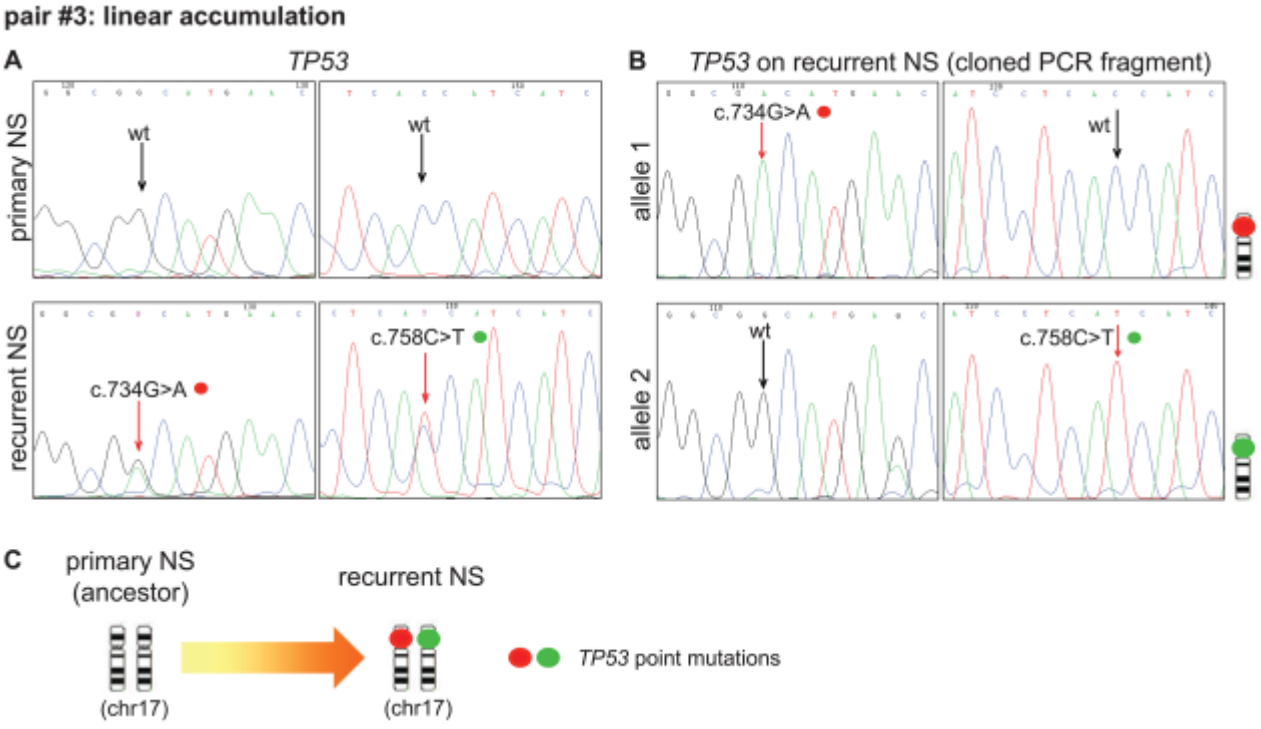

Figure 3. Linear accumulation of TP53 mutations in the recurrent neurosphere (NS) with respect to its matched primary NS (pair #3). (A): Electropherograms representing two TP53 mutations c.734G > A (left) and c.758C > T (right) observed in the recurrent but not in the primary NS. (B): Electropherograms representing the sequence of the TP53 polymerase chain reaction fragment cloned from the recurrent NS, showing that the two mutations (c.734G > A and c.758C > T) occurred on distinct alleles. (C): Schematic representation of the chromosome 17 pair, showing linear accumulation of TP53 mutations in the recurrent with respect to the primary NS. Red arrows: mutated nucleotides; black arrows: wild-type nucleotides. Abbreviations: NS, neurosphere; PCR, polymerase chain reaction; wt, absence of copy number variations.

Pair #4: Divergent Accumulation of Mutations in Primary and Recurrent GSCs

In pair #4, the recurrent NS retained the genetic alterations found in the primary NS, including breast cancer 2 (BRCA2), EGFR, and TP53 mutations, CDKN2A homozygous deletion, and MYC amplification (Fig. 2A; Supporting Information Table S7). Moreover, the recurrent NS acquired mutations potentially affecting protein functions in 41 genes (Fig. 2A, 2B; Supporting Information Table S7). The vast majority of these genetic alterations indicated evolution by linear accumulation as in case #3. However, detailed analysis of TP53 gene (carried out also by Sanger sequencing) suggested a different scenario. While the primary NS harbored a hemizygous TP53 point mutation (c.632C > T), that is, a point mutation in one allele combined with loss of the other allele, the recurrent NS harbored the very same TP53 point mutation as the primary, but in a heterozygous status (i.e., in the presence of a second retained allele, Fig. 4A, 4B), which is incompatible with direct derivation of the recurrent from the primary. Moreover, the recurrent NS accumulated two additional heterozygous point mutations (Fig. 4C–4E). By analysis of 11 different subclones of the recurrent NS, obtained by single-cell cloning, we could show that these three TP53 mutations coexisted in the same cells. By cloning and sequencing (from two cell subclones), the PCR fragment containing the TP53 mutation shared between primary and recurrent NS (c.632C > T, red dot), and one of the two mutations acquired by the recurrent NS (c.565G > A, green dot), we could show that the two mutations occurred in the same allele (Fig. 4F). The relative allelic localization of the second mutation acquired by the recurrent NS (c.451C > T, yellow dot) could not be determined as it was mapped in a different exon.

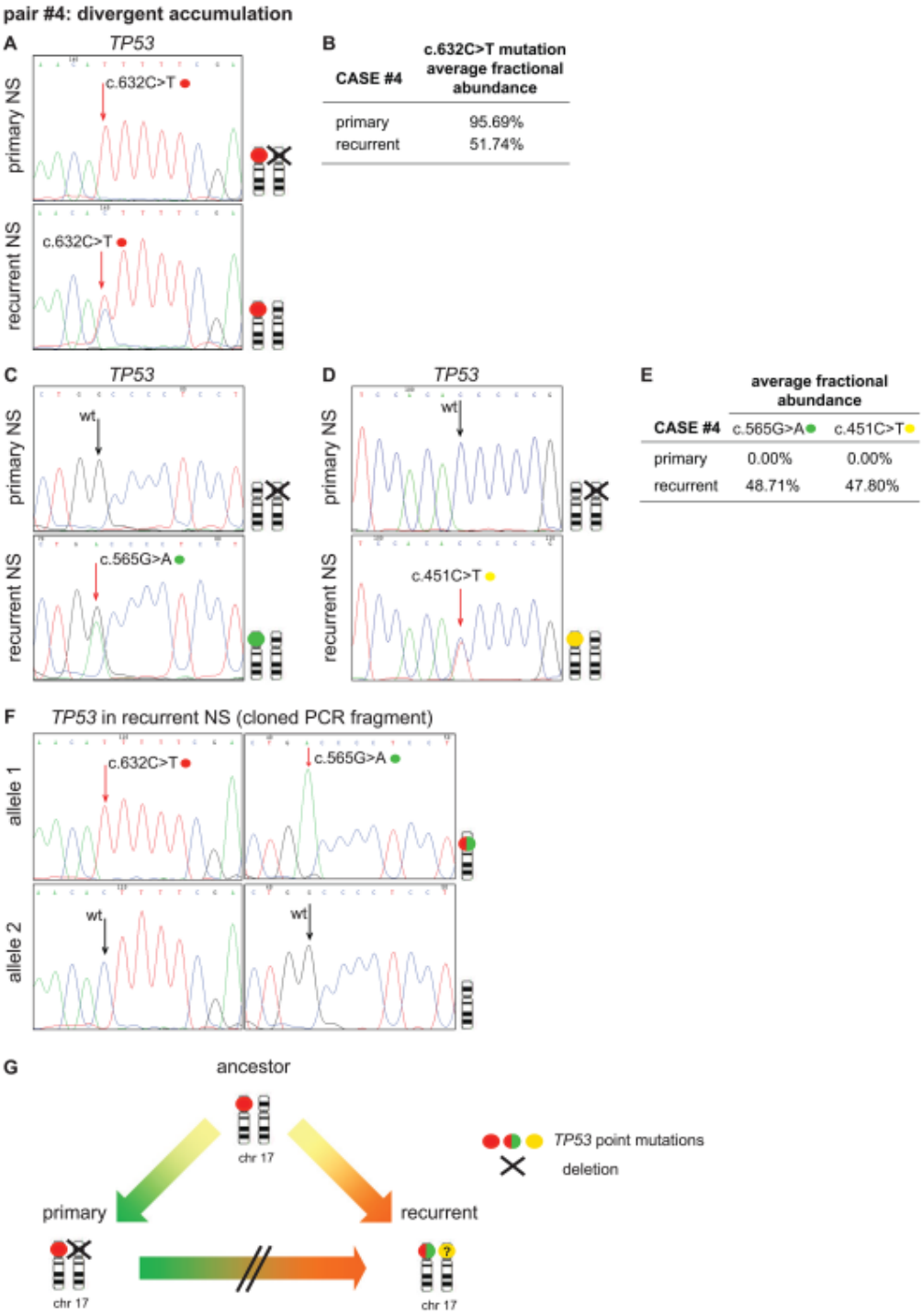

Figure 4. Divergent accumulation of TP53 mutations in the primary and its matched recurrent neurosphere (NS) (pair #4). (A): Electropherograms representing TP53 c.632C > T mutation in a hemizygous status in the primary NS and in a heterozygous status in the recurrent NS. (B)Average fractional abundance of the c.632C > T mutation evaluated in primary and recurrent NS by next generation sequencing (NGS). (C, D): Electropherograms representing TP53mutations c.565G > A (C) or c.451C > T (D), present in a heterozygous status in the recurrent NS but absent from the primary NS. (E): Average fractional abundance of the c.565G > A and c.451C > T mutations, evaluated in primary and recurrent NS by NGS. (F): Electropherograms representing the sequence of the TP53 polymerase chain reaction fragment cloned from the recurrent NS, showing that TP53 mutations c.632C > T and c.565G > A occur on the same allele. (G): Schematic representation of the chromosome 17 pair, showing divergent accumulation of TP53 mutations in the recurrent with respect to the primary NS. The TP53genetic make-up implies that the recurrent NS does not directly derive from the primary, but from a putative common ancestor. Red arrows: mutated nucleotides; black arrows: wild-type nucleotides; colored dots: gene mutations. The allelic assignation of TP53 c.451C > T mutation remains undetermined (question mark, see text). Abbreviations: NS, neurosphere; PCR, polymerase chain reaction; wt, absence of copy number variations.

In summary, as depicted in Figure 4G, these data indicate that the primary and the recurrent NS likely represent GSCs from two genetically distinct subclones that divergently evolved from a common ancestor. This ancestor likely harbored a heterozygous TP53 point mutation (together with CDKN2Ahomozygous deletion, PTEN heterozygous deletion, MYC amplification, BRCA2 and EGFR point mutations, Fig. 2A), which were passed on to both subclones. However, the two subclones underwent divergent accumulation of alterations at least in the TP53 gene (Fig. 4G).

Specific Mutations of Recurrent GSCs Are Already Present in the Primary Tumor

Overall, the analyses of cases #3 and #4 indicated that recurrent NS accumulate genetic alterations over primary NS, providing evidence for either linear or divergent evolution of GSCs from primary to recurrent tumors. As, in recurrent NS, (i) the acquired mutations were associated with a temozolomide genetic signature [19], (ii) and mostly concerned genes rarely mutated in primary GBM [4], we could hypothesize that GSCs isolated from the relapsing tumor were "induced" by temozolomide before being selected. However, we reasoned that TP53 is frequently mutated in primary GBM and could promote resistance against therapy [21]. Thus, we asked whether the tumor subclone expanding in the recurrent tumor was already present before therapy and could be traced by TP53 mutations. Therefore, we measured the average fractional abundance of TP53 mutations in primary tumors. In both cases #3 and #4, the TP53 mutations specific of the recurrent NS (i.e., absent from the primary NS) were found at very low frequency in the primary tumor tissue, (Fig. 5A, 5B). In case #3, each of the two TP53 mutations specific of the recurrent NS displays a ∼50% fractional abundance in NS (consistent with heterozygosity of each mutation, Fig. 3A), and a tiny but significant ∼0.2% in the primary tissue (Fig. 5A). In case #4, the TP53 mutation c.632C > T (red dot), shared by primary and recurrent NS, displays, in the primary NS, an average fractional abundance of ∼100%, indicating that this mutation is hemizygous (consistently with data from sequencing, Fig. 4A, 4B). In the recurrent NS, the frequency of the same mutation drops to ∼50%, consistently with its heterozygous state, as shown by sequencing (Fig. 4A, 4B). Interestingly, the fractional abundance of this TP53 mutation in the primary tissue (∼40%) indicates that the primary tumor can contain multiple subclones harboring this mutation either in hemizygosity, as in the primary NS, or in heterozygosity, as in the recurrent NS and in the putative ancestor (Fig. 5B). The second TP53 mutation c.565G > A (green dot), absent from the primary NS and detectable in the recurrent NS (with a 38% fractional abundance), is present with a ∼0.3% fractional abundance in the primary tissue (Fig. 5B).

A

CASE #3	DNA source	*TP53* mutation average fractional abundance c.734G>A	c.758C>T
primary	tissue	0.255%	0.14%
	NS	0.00%	0.00%
recurrent	NS	52.95%	46.95%

B

CASE #4	DNA source	*TP53* mutation average fractional abundance c.565G>A	c.632C>T
primary	tissue	0.265%	42.5%
	NS	0.00%	95.5%
recurrent II	NS	38%	48.5%

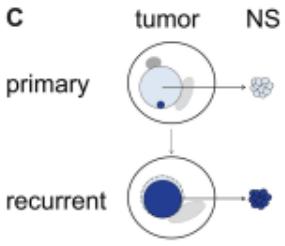

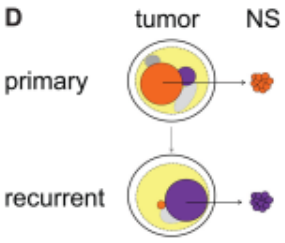

Figure 5. Specific mutations of recurrent neurosphere (NS) are already present in the primary tumor. (A, B): Tables showing the average fractional abundance of the TP53 mutated allele in the primary tissue and in the primary and recurrent NS of case #3 (A) and #4 (B), as determined by droplet digital polymerase chain reaction. (C, D): Schematic representation of the putative, simplified tumor subclonal composition (colored areas) in case #3 (C) and #4 (D). A (minor) subclone coexists with one or more other genetically related subclones in the primary tumor, survives therapies, and expands in the recurrent. Different colors indicate genetically distinct subclones; case #4 (D), yellow: presumptive common ancestor. Primary and recurrent NS reflect the genetic make-up of single tumor subclones. Abbreviation: NS, neurosphere.

In both cases #3 and #4, the presence—in primary tumor tissues—of TP53 mutations distinctive of recurrent NS indicates that subclones expanding in recurrent tumors were already present before mutagenic chemoradiotherapy. likely, TP53 mutation itself could confer to these subclones an inherent selective advantage under therapeutic pressure [21] (Fig. 5C, 5D).

Recurrent GSCs Display Greater Therapeutic Resistance than Primary GSCs

We then asked whether, in cases where genetic evolution was observed, primary and recurrent NS display different aggressiveness and sensitivity to therapies administered to patients after surgery. Therefore, the basal proliferation rate, the tumorigenic potential and the response to chemoradiotherapy of primary and recurrent NS (pair #3 and #4) were compared (Fig. 6A–6H). As expected, an increased proliferation rate and tumorigenic potential was displayed by both recurrent NS with respect to their matched primary NS (Fig. 6A–6D). Then, NS viability was measured in time-course experiments after fractionated doses of ionizing radiation (2 Gy × 3 days) (Fig. 6E, 6F). In pair #3, both primary and recurrent NS displayed a similar radiosensitivity (Fig. 6E). This can be explained by the fact that the patient did not receive radiotherapy, and thus the recurrent tumor arose from GSCs that were not exposed to such therapeutic pressure. On the contrary, in pair #4, isolated from a patient that received radiotherapy, the recurrent NS, although still sensitive to irradiation, was significantly more resistant than the primary (Fig. 6F). Finally, NS viability in response to temozolomide was measured in time-course (up to 10 days) and dose–response experiments (Fig. 6G, 6H; Supporting Information Fig. S3). In both cases, while primary NS were very sensitive to the drug, recurrent NS were strongly resistant, supporting the conclusion that recurrent GSCs were positively selected by chemotherapy. As shown above, the selective pressure likely favored a pre-existing tumor subclone endowed with inherent resistance conferred by TP53 mutations [21]. However, the temozolomide refractoriness of recurrent NS could be explained also by acquisition of more direct mechanisms of resistance alternative to MGMT expression (that remained negative in the recurrent NS, Fig. 2A), such as the inactivating mutations of mismatch repair genes [22] MSH2 (case #3) and MSH6 (case #4) (Fig. 2A; Supporting Information Tables S6A, S7A).

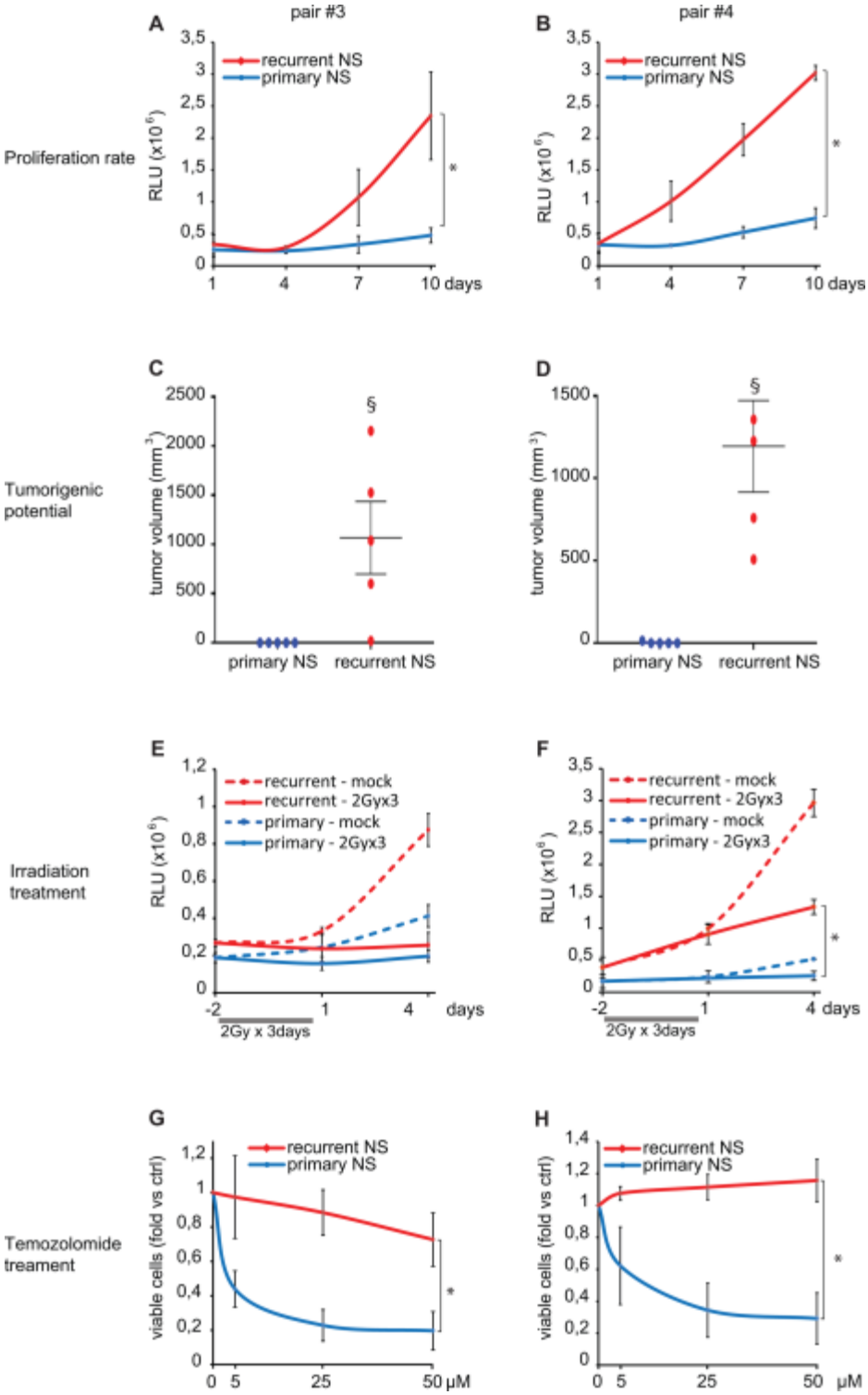

Figure 6. Proliferation rate, tumorigenic potential, and therapeutic resistance of primary and recurrent neurospheres (NS). (A, B): Cell viability evaluated at the indicated time points after seeding. Data are shown as mean ± SEM, n = 12. (C, D): Tumor volume measured when xenografts from recurrent NS reached the experimental endpoint [15 weeks, (C); 9 weeks, (D)]. Data are shown as mean ± SEM, n = 5 per group. (E, F): Cell viability measured at the indicated time points after the last irradiation (2 Gy × 3 days). Data shown are from a representative experiment (n = 12) and are mean ± SEM. Mock: nonirradiated control cells. (G, H): Cell viability measured 3 days after the third and last temozolomide administration at the indicated doses. Data (fold vs. mock-treated cells, ctrl) are shown as mean ± SEM, n = 12. *, p <.01 (t-test; primary vs. recurrent); §, p <.01 (Mann Whitney test). Abbreviations: NS, neurosphere; RLU, relative luciferase unit.

Discussion

Cancer stem-like cells (CSCs) have been recognized as the origin of tumor phenotypic heterogeneity, that is, the formation of a cell hierarchy that includes a (tiny) subset of cells endowed with self-renewal and tumorigenic properties, which regenerates itself and a (major) subset of pseudo-differentiating cells, which lose tumorigenic along with stem properties [23]. So far, little attention has been turned to the fact that CSCs should reflect progressive accrual of genetic lesions within the tumor, that is, that they lie at the roots of cancer genetic heterogeneity. However, compelling interpretation of findings in leukemia has led to the concept that CSCs are the "units of cancer clonal evolution" [24, 25]. According to this view, CSCs must accumulate the driving genetic alterations, responsible for the phenotypic traits on which the selective pressure of the environment operates and promotes genetic evolution. Among these selective pressures, the one exerted by chemoradiotherapy is powerful, and favors the emergence of CSCs harboring the genetic determinants of therapeutic resistance, that generate tumor subclones originating tumor recurrence.

The limited knowledge about CSC genetics, and in particular about their evolutionary dynamics under selective pressure, is partly justified by technical hitches in obtaining CSCs from multiple, genetically distinct areas of a single tumor, and from pairs of matched primary and recurrent/metastatic tumors. These difficulties concern also GBM CSCs (GSCs) for two reasons: (a) GBM invariably relapses but, only in a minority of cases, it undergoes second or third surgery, obviously required to recover the tissue for GSC derivation as NS; (b) the possibility to actually establish a NS from each surgical sample is, in our experience of hundreds of cases, usually around 50%–65%. In this study, we could tackle the challenging goal of investigating GSC genetic evolution, by taking advantage of a few pairs of NS previously isolated from matched primary and recurrent tumors. The latter arose after the standard therapeutic protocol was applied to the primary tumor, including surgery followed by chemoradiotherapy, which likely imposed a selective pressure on residual, often numerous and infiltrating cells. Thus, the recurrent GBM expanded from GSCs harboring determinants of resistance, which are mostly associated with hereditable genetic factors.

To investigate GSC genetic evolution under therapeutic pressure, we analyzed an ample panel of cancer-associated genes by NGS, including all the main GBM genetic drivers. In two out of four cases (#3 and #4), this analysis allowed to trace genealogical relationships among GSCs isolated from primary and recurrent tumors, showing linear or divergent accrual of genetic alterations in recurrent GSCs as compared with primary GSCs.

Importantly, by considering the relative frequency of genetic variants observed in NGS analysis, we could confirm the expected genetic homogeneity, that is, the monoclonality, of each and every NS, which therefore should contain the GSCs that originate a single tumor subclone. Despite the limited size of the surgical specimen from which NS were derived, we can hypothesize that the primary NS contains GSCs that originate the subclone prevailing in the primary tumor, while the recurrent NS contain GSCs that survived therapies and expanded in the relapsing tumors.

Notably, in case #4, the genealogic relationship between primary and recurrent GSCs, traced by detailed analysis of TP53 mutations, can be explained only by inferring the presence of an ancestor common to both GSCs. This presumptive ancestor GSC was not isolated as NS from the primary tumor, either because not included in the surgical sample or negatively selected during derivation.

Importantly, in both cases showing genetic evolution, analysis of TP53 mutations in NS and primary tumor tissues revealed that the subclone (and thus the GSC) that expanded in the recurrent tumor, was already present in the primary, before the selective pressure of chemoradiotherapy was exerted. This is reminiscent of findings in lung and colorectal cancer, where minor subclones, harboring a genetic determinant of resistance against a therapeutic agent, pre-exist in the primary tumor and drive the recurrence after being positively selected by therapy [26, 27]. In our cases, it is difficult to establish to which extent the TP53 genetic alterations, distinctively marking the recurrent GSCs, play a role as a genetic determinant of resistance to the selective pressure applied by chemoradiotherapy (and anti-angiogenic therapy in case #4). Remarkably, however, genetic evolution of recurrent GSCs reflects also accrual of genetic alterations likely induced by the mutagenic effect of temozolomide. Indeed, genetic evolution is observed only in the two cases (#3 and #4) whose primary tumors do not express MGMT. As result, these tumors fail to counteract therapy-induced DNA alkylation, but can also suffer from constitutive genetic instability [28], which explains the appearance of TP53 mutant

subclones prior to therapy. Mutations accumulated in recurrent GSCs display the “temozolomide signature” [19] and involve genes not listed among the common GBM genetic drivers, but including mismatch repair genes [22], which are expected to confer a further selective advantage that sustain expansion in the recurrence. In summary, this study enlightens the occurrence of linear or branching genetic evolution in GSCs from primary to recurrent tumor, and indicates that the complex architectures observed in whole-tissue GBMs are reflected at the GSC level and shaped by therapeutic pressure.

Conclusion

By comparing the mutational profile of matched NS (cultures enriched in GSCs) derived from primary or recurrent GBM, GSC genetic evolution can be observed.

Recurrent GSCs are phylogenetically related with primary GSCs, and can accumulate mutations following linear or divergent pathways, mirroring genetic evolution of the original tumor subclones.

GSCs giving rise to recurrent tumors pre-exist in the primary, are likely selected by therapeutic pressure, and can concomitantly accumulate further genetic alterations for the mutagenic effect of therapies, especially temozolomide.

Acknowledgments

We thank Marica Eoli for clinical information, Monica Patané and Bianca Pollo for providing glioblastoma tissues, Alberto Bardelli for discussion, Raffaella Albano, Alice Bartolini, and Stefania Bolla for technical help, Antonella Cignetto, Daniela Gramaglia, and Francesca Natale for secretarial assistance. This work was supported by AIRC, Italian Association for Cancer Research (“Special Program Molecular Clinical Oncology 5xMille, N. 9970”; IG 15709 [to C.B.], 13043 [to G.F.], and 15572 [to P.M.C.]); Italian Ministry of Health (Ricerca Corrente); and Comitato per Albi98.

Author Contributions

F.O. and F.D.B: conception and design, collection of data, data analysis and interpretation, and manuscript writing; G.C.: data analysis and interpretation; S.P.: provision of study material; B.M. and G.S.: data collection and analysis; A.D.A.: in vivo experiments, data analysis and interpretation; P.M.C.: financial support and final approval of manuscript; G.F.: provision of study material, financial support and final approval of manuscript; C.B.: conception and design, data analysis and interpretation, manuscript writing, financial support, and final approval of manuscript.

Disclosure of Potential Conflicts of Interest

The authors indicated no potential conflicts of interest.

References

1. Louis DN, Perry A, Reifenberger G et al. The 2016 World Health Organization classification of tumors of the central nervous system: A summary. Acta Neuropathol 2016;131:803–820.

2. Snuderl M, Fazlollahi L, Le LP et al. Mosaic amplification of multiple receptor tyrosine kinase genes in glioblastoma. Cancer Cell 2011;20:810–817.

3. Sottoriva A, Spiteri I, Piccirillo SG et al. Intratumor heterogeneity in human glioblastoma reflects cancer evolutionary dynamics. Proc Natl Acad Sci USA 2013;110:4009–4014.

4. Brennan CW, Verhaak RG, McKenna A et al. The somatic genomic landscape of glioblastoma. Cell2013;155:462–477.

5. Johnson BE, Mazor T, Hong C et al. Mutational analysis reveals the origin and therapy-driven evolution of recurrent glioma. Science 2014;343:189–193.

6. Wang J, Cazzato E, Ladewig E et al. Clonal evolution of glioblastoma under therapy. Nat Genet 2016;48:768–776.

7. Kim J, Lee IH, Cho HJ et al. Spatiotemporal evolution of the primary glioblastoma genome. Cancer Cell2015;28:318–328.

8. Kim H, Zheng S, Amini SS et al. Whole-genome and multisector exome sequencing of primary and post-treatment glioblastoma reveals patterns of tumor evolution. Genome Res 2015;25:316–327.

9. Bao S, Wu Q, McLendon RE et al. Glioma stem cells promote radioresistance by preferential activation of the DNA damage response. Nature 2006;444:756–760.

10. Chen J, Li Y, Yu TS et al. A restricted cell population propagates glioblastoma growth after chemotherapy. Nature 2012;488:522–526.

11. De Bacco F, D'ambrosio A, Casanova E et al. MET inhibition overcomes radiation resistance of glioblastoma stem-like cells. EMBO Mol Med 2016;8:550–568.

12. Piccirillo SG, Combi R, Cajola L et al. Distinct pools of cancer stem-like cells coexist within human glioblastomas and display different tumorigenicity and independent genomic evolution. Oncogene 2009;28:1807–1811.

13. Piccirillo SG, Colman S, Potter NE et al. Genetic and functional diversity of propagating cells in glioblastoma. Stem Cell Rep 2015;4:7–15.

14. Stieber D, Golebiewska A, Evers L et al. Glioblastomas are composed of genetically divergent clones with distinct tumourigenic potential and variable stem cell-associated phenotypes. Acta Neuropathol 2014;127:203–219.

15. Louis DN, Ohgaki H, Wiestler OD et al. The 2007 WHO classification of tumours of the central nervous system. Acta Neuropathol 2007;114:97–109.

16. De Bacco F, Casanova E, Medico E et al. The MET oncogene is a functional marker of a glioblastoma stem cell subtype. Cancer Res 2012;72:4537–4550.

17. Siravegna G, Mussolin B, Buscarino M et al. Clonal evolution and resistance to EGFR blockade in the blood of colorectal cancer patients. Nat Med 2015;21:795–801.

18. Chen L, Liu P, Evans TC et al. DNA damage is a pervasive cause of sequencing errors, directly confounding variant identification. Science 2017;355:752–756.

19. Alexandrov LB, Nik-Zainal S, Wedge DC et al. Signatures of mutational processes in human cancer. Nature2013;500:415–421.

20. Van Emburgh BO, Arena S, Siravegna G et al. Acquired RAS or EGFR mutations and duration of response to EGFR blockade in colorectal cancer. Nat Commun 2016;7:13665.

21. Dinca EB, Lu KV, Sarkaria JN et al. p53 Small-molecule inhibitor enhances temozolomide cytotoxic activity against intracranial glioblastoma xenografts. Cancer Res 2008;68:10034–10039.

22. Fu D, Calvo JA, Samson LD. Balancing repair and tolerance of DNA damage caused by alkylating agents. Nat Rev Cancer 2012;12:104–120.

23. Kreso A, Dick JE. Evolution of the cancer stem cell model. Cell Stem Cell 2014;14:275–291.

24. Greaves M. Cancer stem cells: Back to Darwin? Semin Cancer Biol 2010;20:65–70.

25. Greaves M. Evolutionary determinants of cancer. Cancer Discov 2015;5:806–820.

26. Turke AB. Preexistence and clonal selection of MET amplification in EGFR mutant NSCLC. Cancer Cell2010;17:77–88.

27. Misale S, Yaeger R, Hobor S et al. Emergence of KRAS mutations and acquired resistance to anti-EGFR therapy in colorectal cancer. Nature 2012;486:532–536.

28. Cabrini G, Fabbri E, Lo Nigro C et al. Regulation of expression of O6-methylguanine-DNA methyltransferase and the treatment of glioblastoma. Int J Oncol 2015;47:417–428.